

**The influence of
vegetation dynamics
on anthropogenic
climate change**

U. Port et al.

The influence of vegetation dynamics on anthropogenic climate change

U. Port¹, V. Brovkin¹, and M. Claussen^{1,2}

¹Max-Planck Institute for Meteorology in Hamburg, Hamburg, Germany

²Meteorological Institute, KlimaCampus, University of Hamburg, Hamburg, Germany

Received: 15 June 2012 – Accepted: 26 June 2012 – Published: 5 July 2012

Correspondence to: U. Port (ulrike.port@zmaw.de)

Published by Copernicus Publications on behalf of the European Geosciences Union.

Title Page

Abstract

Introduction

Conclusions

References

Tables

Figures

⏪

⏩

◀

▶

Back

Close

Full Screen / Esc

Printer-friendly Version

Interactive Discussion

Abstract

In this study, vegetation-climate and vegetation-carbon cycle interactions during anthropogenic climate change are assessed by using the Earth System Model MPI ESM including a module for vegetation dynamics. We assume anthropogenic CO₂ emissions according to the RCP 8.5 scenario in the period from 1850 to 2120 and shut them down afterwards to evaluate the equilibrium response of the Earth System by 2300.

Our results suggest that vegetation dynamics have a considerable influence on the changing global and regional climate. In the simulations, global mean tree cover extends by 2300 due to increased atmospheric CO₂ concentration and global warming. Thus, land carbon uptake is higher and atmospheric CO₂ concentration is lower by about 40 ppm when considering dynamic vegetation compared to a static pre-industrial vegetation cover. The reduced atmospheric CO₂ concentration is equivalent to a lower global mean temperature. Moreover, biogeophysical effects of vegetation cover shifts influence the climate on a regional scale. Expanded tree cover in the northern high latitudes results in a reduced albedo and additional warming. In the Amazon region, declined tree cover causes a higher temperature as evapotranspiration is reduced. In total, we find that vegetation dynamics have a slight attenuating effect on global climate change as the global climate cools by 0.22 K in 2300 due to natural vegetation cover shifts.

1 Introduction

Atmospheric CO₂ concentrations and climate changes projected for the 21st century (Meehl et al., 2007) are unprecedented in the geological history of the last several million years. Since the geographical distribution of natural plants is controlled by climate, to large extent (Woodward and Beerling, 1997), spatial distribution of vegetation types will be modified in response to climatic changes. In addition, elevated atmospheric CO₂ concentration acts as a fertiliser for the biosphere. Plant productivity and water-use

ESDD

3, 485–522, 2012

The influence of vegetation dynamics on anthropogenic climate change

U. Port et al.

Title Page

Abstract

Introduction

Conclusions

References

Tables

Figures

⏪

⏩

◀

▶

Back

Close

Full Screen / Esc

Printer-friendly Version

Interactive Discussion



efficiency becomes higher under increasing atmospheric CO₂ conditions until saturation is reached (de Boera et al., 2011). This fertilisation effect leads to extended plant growth and alters the competition among plants.

The response of the terrestrial biosphere to anthropogenic climate change has already been detected in satellite and phenological data. Myneni et al. (1997), Menzel and Fabian (1999), and Zhou et al. (2001) observe increased plant growth in the northern high and mid latitudes (45° N to 70° N) from the 1980s to the 1990s due to extending growing seasons. Piao et al. (2011) and Beck and Goetz (2011) analyse satellite data for the period from 1986 until 2006 and find increasing plant growth in the tundra region over the whole period. However, a decreasing trend in plant growth occurs in the boreal region from 1996 until 2006.

As the biosphere influences energy, water, and gas fluxes, shifts in plant distribution will in turn lead to changes in regional and global climate. Two different effects by which the vegetation affects climate can be distinguished, the biogeophysical and the biogeochemical effect. The biogeophysical effect refers to the impact of vegetation on the energy, the moisture, and the momentum fluxes due to its physical properties such as leaf area, albedo, and roughness length (Claussen et al., 2001). The biogeochemical effect represents the impact of the biosphere on the chemical composition of the atmosphere. In this study, we refer the biogeochemical effect only to the influence on the atmospheric CO₂ concentration. The biosphere affects land carbon uptake and the atmospheric CO₂ concentration since it builds up biomass.

In recent years, climate models coupled to land surface models have become a common tool to assess the influence of the biosphere on the climate. Two different main effects of forests on the climate have been found depending on the region. In the tropics, forests lead to a reduced albedo and an enhanced evapotranspiration compared to bare soil. The albedo reduction is equivalent to a warming, while increased evapotranspiration leads to a cooling. In sum, the cooling outweighs the warming, and forests cool the tropical climate (Snyder et al., 2004).

The influence of vegetation dynamics on anthropogenic climate change

U. Port et al.

Title Page

Abstract

Introduction

Conclusions

References

Tables

Figures



Back

Close

Full Screen / Esc

Printer-friendly Version

Interactive Discussion



The influence of vegetation dynamics on anthropogenic climate change

U. Port et al.

Title Page

Abstract

Introduction

Conclusions

References

Tables

Figures



Back

Close

Full Screen / Esc

Printer-friendly Version

Interactive Discussion



Unlike tropical forests, boreal forests are suggested to warm climate, since they cover the snow and thus reduce surface albedo strongly compared to herbaceous vegetation and low-stand shrubs (Brovkin, 2002; Essery et al., 2009). The impact of temperate forests on climate depends on the seasons. In winter and spring, temperate forests warm the regional climate by reducing the albedo, while in summer they cool the climate by increasing the latent heat flux. On a global scale, the biogeophysical effect of forests is likely to lead to a warmer climate as the cooling effect of enhanced transpiration in the tropics is weaker than the warming effect of reduced land surface albedo in the high latitudes (Brovkin et al., 2009).

Taking the biogeochemical effect into account as well modifies the net impact of forest on climate. In idealised deforestation/afforestation experiments, model simulations show that forests cause a cooler climate in the tropics, since tropical forests take up large amounts of carbon. The resulting cooling further enhance the cooling due to increased evapotranspiration (Claussen et al., 2001; Bala et al., 2007; Bathiany et al., 2010). For forests in the high and mid latitudes, the biogeochemical and the biogeophysical effects counteract. Biomass build up by forest tends to cool climate, while the albedo reduction due to forest leads to a warmer climate. In balance, the albedo effect is stronger and high and mid latitude forests warm regional climate.

Because of the interactions between the terrestrial biosphere and the atmosphere, changes in distribution of vegetation cover (vegetation dynamics) need to be considered when simulating anthropogenic climate change. Based on simulations made with Global Dynamic Vegetation Model (DGVM) coupled to Atmospheric General Circulation Models (AGCMs), the shifts in vegetation cover due to an increased atmospheric CO₂ concentration and the resulting influence on the climate (Notaro et al., 2007; O'ishi and Abe-Ouchi, 2009; Yurova and Volodin, 2011) and on the carbon cycle (Jones et al., 2010) have been assessed. Notaro et al. (2007) assume four times pre-industrial atmospheric CO₂ concentrations and find that increased temperatures in the northern high latitudes lead to a northward expansion of boreal forests. The extended tree cover leads further warming since the surface albedo is reduced. For the respond of the

The influence of vegetation dynamics on anthropogenic climate change

U. Port et al.

Title Page

Abstract

Introduction

Conclusions

References

Tables

Figures

⏪

⏩

◀

▶

Back

Close

Full Screen / Esc

Printer-friendly Version

Interactive Discussion



Amazonian forest, simulation results differ. Depending on the changes in the general atmospheric circulation Cox et al. (2004), Betts et al. (2004), and Notaro et al. (2007) find a decreasing tree cover since the regional climate becomes too dry. The resultant reduction in evapotranspiration leads to a further drying. However, Yurova and Volodin (2011) simulates no forest degradation in the Amazon region as soil moisture remains sufficient to maintain forest growth. The simulated vegetation cover changes due to future climate change are suggested to influence the carbon cycle.

In our study, we assess the biogeographical changes due to anthropogenic CO₂ emissions and the resulting climate change based on model simulation performed with the Earth System Model MPI ESM including a dynamic vegetation module and an interactive carbon cycle. Furthermore, the impact of vegetation dynamics on climate is estimated by separating the biogeophysical and biogeochemical effect. We assume a transient CO₂ emission scenario according to the Representative Concentration Pathway 8.5 (RCP 8.5) until the year 2120 and set the CO₂ emissions to zero afterwards. The simulations continue until 2300. Analysing the impact of vegetation dynamics on climate change on a time scale of several centuries is unique.

The results are presented and discussed in tree steps. First, the simulated climate changes and the subsequent shifts in vegetation cover until 2120 are examined, followed by the anthropogenic climate changes as well as biogeographical shifts by the year 2300. In the third step, the impact of vegetation dynamics on the regional and the global climate as well as on the carbon cycle are analysed. Thereby, the biogeophysical and the biogeochemical effect are regarded separately.

2 Model setup and methods

The Earth System Model of the Max-Planck Institute for Meteorology (MPI ESM) employed here consists of the Atmospheric General Circulation Model (AGCM) ECHAM5 (Roeckner et al., 2003), the Jena Scheme for Biosphere Atmosphere Coupling in Hamburg (JSBACH) (Raddatz et al., 2007), the ocean model Max-Planck Institute Ocean

The influence of vegetation dynamics on anthropogenic climate change

U. Port et al.

Title Page

Abstract

Introduction

Conclusions

References

Tables

Figures



Back

Close

Full Screen / Esc

Printer-friendly Version

Interactive Discussion



Model (MPI-OM) (Jungclaus et al., 2006), and the ocean biogeochemistry model HAMOCC5 (Wetzel et al., 2005). All components are connected with each other in an interactive carbon cycle. ECHAM5 runs in a T31 resolution (approx. 3.75°) with 19 vertical levels. The grid of the ocean model has a resolution of about 3° and 40 levels. JSBACH includes a dynamic vegetation module based on a tiling approach (Brovkin et al., 2009). The vegetation is represented by the eight Plant Functional Types (PFTs) listed in Table 1. For the analysing process, these PFTs are further grouped into forest, shrubs, and grass.

Four simulation were performed as listed in Table 2. The control simulation (CTL) runs without anthropogenic CO_2 emissions. The atmospheric CO_2 concentration varies around 275 ppm and the climate is in equilibrium. The equilibrium vegetation distribution is depicted in Fig. 1. The simulated tree cover distribution matches observations based on satellite data in the main boreal and temperate pattern (Brovkin et al., 2009).

The STAT simulation is forced by CO_2 emissions according to the anthropogenic CO_2 emissions included in the Representative Concentration Pathway 8.5 scenario (RCP 8.5). The emissions last until 2120 and and accumulate to 3000 Pg Carbon by 2120. Afterwards, the simulation continues without CO_2 emissions until 2300. The vegetation cover is held constant at the equilibrium distribution of the control simulation. However, the plant productivity and canopy conductance respond to the increased atmospheric CO_2 concentrations. Differences in the climate between the STAT and the CTL simulation reflect the climate change due to the CO_2 emissions and plant physiological changes.

The third simulation, referred to as DYN simulation, is driven by the same CO_2 emissions as the STAT simulation (CO_2 emission according to the RCP 8.5 scenario until 2120 and zero emissions afterwards until 2300). The vegetation cover changes dynamically due to increased atmospheric CO_2 concentrations and climate change. Vegetation cover shifts due to land-use are neglected. Regarding climate, differences between the DYN and the STAT simulation can be attributed to biogeographical shifts and differences in plant productivity and canopy conductance.

The influence of vegetation dynamics on anthropogenic climate change

U. Port et al.

Title Page

Abstract

Introduction

Conclusions

References

Tables

Figures



Back

Close

Full Screen / Esc

Printer-friendly Version

Interactive Discussion



In the STAT_PS simulation, the atmospheric CO₂ concentration is set to the values calculated in the DYN simulation. The vegetation distribution is fixed to the equilibrium of the CTL simulation. Plant productivity and canopy conductance respond to changed environmental conditions. When comparing the DYN and the STAT_PS simulation, climate changes are caused by the different physiological response of the plants and biogeographical changes. Since the climate changes due to the different plant productivity and canopy conductance are very much smaller than the changes due to the vegetation cover shifts, we neglect the climate changes due to the physiological response of the plants. Thus, the climate changes between the DYN and the STAT_PS simulation are assumed to be caused by the biogeophysical shifts alone.

The changes of the biogeographical distribution can be subdivided into two periods. The first period lasts from the year 1850 until 2120, when atmospheric CO₂ concentration increases and climate changes rapidly. During this time, CO₂ fertilisation and climate change act on the biosphere simultaneously. The second period starts in 2120, when the CO₂ emissions are switched off. From 2120 until 2300, atmospheric CO₂ concentration declines, CO₂ fertilisation weakens, and climate tends to stabilise. Climate change and subsequent changes in the terrestrial biosphere are presented for these two periods.

Since the vegetation cover changes are strongest at the end of the simulation, the impact of these changes on climate and on the carbon cycle are analysed in detail averaged over the last 30 yr of the simulations (2270–2300).

Analysis focuses on the global and on the regional effect of vegetation cover changes on the climate and the carbon cycle. The regions chosen for detailed analysis are the northern high latitudes, the Amazon region, and the Sahara. The northern high latitudes encompass the area north of 60° N up to 80° N. The Amazon region and the Sahara are defined as the area from 70° W to 50° W and from 15° S to the equator and as the area from 20° W to 45° E and from 10° N to 35° W, respectively.

3 Results and discussion

3.1 Changes in climate and vegetation cover during the emission period (1850–2120)

The extension of the RCP 8.5 scenario used here implies that 3000 PgC are emitted until the year 2120. In response to these CO₂ emissions, the atmospheric CO₂ concentration in the DYN simulation is larger by 592.1 ppm (averaged from the year 2070 until 2119) than in the control run (Fig. 2). Global annual mean temperature and precipitation increase by 4.4 K and 0.18 mm day⁻¹ (~ 6.6 %), respectively.

The strongest warming occurs in the northern high latitudes (Fig. 3). Between 60°N and 80°N, the annual mean temperature rises by 8.1 K (averaged from 2090 until 2119). This polar amplification is caused by the ice-albedo feedback and changes in the Bowen ratio (McBean et al., 2005) and is found in previous future climate simulations as well (Meehl et al., 2007). The warming over land is stronger than over the oceans, consistent with Meehl et al. (2007). Warming over the equatorial oceans exceeds warming over the North Atlantic, North Pacific, and Southern Ocean. These differences in warming are partly caused by a reduced oceanic heat transport. The Atlantic Meridional Ocean Circulation (AMOC) at 26° N weakens by 3.3 Sv by 2120.

Precipitation changes over land are weaker than over the ocean (Fig. 4). Precipitation increases over land occur in parts of western North America, Siberia, and western South America. Precipitation decreases in Australia as well as in parts of the Amazon region.

Global mean continental area not covered by vegetation, including deserts and glaciers, shrinks from 27 % to 23 % averaged from 2090 to 2119, while tree and grass benefit from changed climate conditions and increased atmospheric CO₂ concentration (Fig. 5). On a regional scale, vegetation cover expands and desert area shrinks in nearly all regions (Fig. 6). Tree and shrubs cover increase in the Sahara and Central Asia and grass cover increases in Australia. In the northern high latitudes, tree cover increases. Trees succeed grass in Alaska, while they substitute shrubs in Siberia.

The influence of vegetation dynamics on anthropogenic climate change

U. Port et al.

Title Page

Abstract

Introduction

Conclusions

References

Tables

Figures



Back

Close

Full Screen / Esc

Printer-friendly Version

Interactive Discussion



Climate change results in declining tree cover in the Amazon region, where tree cover shrinks from 73% absolute coverage to 60% until the year 2120. The trees are replaced by grass, which extends by the same amount of 13% area coverage.

In the period from 1850 until 2120, CO₂ fertilisation and changed climate conditions act simultaneously on the terrestrial biosphere. Changes in Net Primary Production (NPP) between the STAT and the control simulation reflect the influence of the CO₂ fertilisation on photosynthesis rate and biomass build up. NPP increases nearly all over the globe by the year 2120 (Fig. 8). In contrast, warmer conditions lead to a reduced NPP in the Amazon region. Other than in the mid and high latitudes, where plant growth is dominated by temperature, water availability limits plant growth in the tropics and subtropics. Therefore, NPP is more sensitive to water stress in the tropics than in the high and mid latitudes. Higher temperatures lead to a stronger water stress and a decreased NPP. Thus, the warming by 6.6 K in the Amazon region overcompensates CO₂ fertilisation resulting in the tree cover decline by 13% absolute coverage.

As this decline in tree cover depends on water stress, it differs from the forest dieback found in previous studies. Using the IS92a CO₂ emission scenario, Betts et al. (2004) simulate a decline in precipitation of 60% causing a forest dieback from 80% to 10% absolute coverage during the 21st century. In our simulations, precipitation change is smaller compared to Betts et al. (2004) resulting in a weaker forest cover decline.

NPP remains constant in desert regions, where water is rare and limits plant growth. However, NPP increases at the border of the deserts in the Sahara, the Middle East, Australia, and subtropic South America. As water stress is weaker in these regions than in the central desert areas, increased water-use efficiency becomes effective and NPP rises.

In short, CO₂ fertilisation causes an increased NPP and leads to extended tree and grass cover in all regions, where climate conditions are favourable (northern high latitudes, Central Asia, and the borders of the large deserts). However, CO₂ fertilisation becomes non-effective in regions of stronger water stress due to elevated temperatures (in parts of the Amazon region and central desert regions).

The influence of vegetation dynamics on anthropogenic climate change

U. Port et al.

Title Page

Abstract

Introduction

Conclusions

References

Tables

Figures



Back

Close

Full Screen / Esc

Printer-friendly Version

Interactive Discussion



The influence of vegetation dynamics on anthropogenic climate change

U. Port et al.

Title Page

Abstract

Introduction

Conclusions

References

Tables

Figures



Back

Close

Full Screen / Esc

Printer-friendly Version

Interactive Discussion



These findings are in line with previous studies. Bala et al. (2006) find a global mean increase in tree cover and a decline in grass and shrubland cover due to CO₂ fertilisation assuming the SRES A2 CO₂ emission scenario. The continental deserts are replaced by trees and boreal forests extend northward in their simulations. In sensitivity studies on the physiological effect of elevated atmospheric CO₂ on global vegetation cover by Bala et al. (2006), Notaro et al. (2007), and O'ishi and Abe-Ouchi (2009), the strongest influence of CO₂ fertilisation on vegetation has been found in moisture-limited regions, where increased water-use efficiency leads to extended plant growth.

Besides the CO₂ fertilisation effect, extended growing periods facilitate boreal forests to expand in the northern high latitudes by the year 2120. Mean temperature over land increases by 8.3 K in the northern high latitudes averaged from 2090 until 2119 (DYN – CTL). Especially winters become warmer, as the mean temperature in January increases by 15 K over land. The warming in spring and autumn shortens the period with snow covering the ground. Hence, vegetation growth becomes more suitable during this time and the growth season extends. Furthermore, precipitation increases by 29 % (DYN – CTL) leading to a larger amount of water available for plant growth.

The vegetation cover in the Sahel zone responds to CO₂ fertilisation, but also depends on precipitation. Figure 9 illustrates the time series for changes in vegetation cover and in annual mean precipitation in the Sahara. Precipitation over land averaged from the year 2060 until 2089 increases by 20 % related to the control simulation (DYN – CTL). In combination with the CO₂ fertilisation, the higher precipitation rate leads to an increase in tree and shrubs cover from 7 % to 10 % and 3 % to 5 % respectively until 2089 (averaged from 2060 until 2089). Thus, the desert area shrinks from 77 % to 72 % absolute coverage. From 2090 on, precipitation declines and temperature continues to increase. The desert area increases instantaneously due to the resulting water stress. Thereby, shrubs and grass cover decline, while tree cover still increases.

3.2 Changes in climate and vegetation cover during climate stabilisation (2120–2300)

After the abrupt end of emissions in 2120, atmospheric CO₂ concentration declines with a decay rate of 1.5 ppm yr⁻¹ and 0.9 ppm yr⁻¹ from 2120 until 2200 and from 2200 until 2300 in the DYN simulation, respectively (Fig. 2). At the end of the simulation, the atmospheric CO₂ concentration is 497 ppm above the pre-industrial value. The global annual mean temperature and precipitation continue to increase until about the year 2150. From 2200 until 2300, the global annual mean temperature reveals no significant trend, while global annual mean precipitation declines slightly (0.0014 mm day⁻¹ in 100 yr). the global mean temperature and precipitation in DYN are 5.6 K and 0.3 mm day⁻¹ (~ 10 %) higher than in the control run by 2300.

The temperature further rises by 1.3 K in the northern high latitudes from 2120 until 2300 (Fig. 10). The weakest warming occurs over the North Atlantic Ocean. The AMOC declines by a further 4 Sv at 26° N and 1000 m depth from 2120 to 2300 leading to a weaker heat transport from the low to the high latitudes. Over land no further significant changes in precipitation occur from 2120 to 2300.

The global mean continental area not covered by vegetation increases slightly and shrubs as well as grass cover shrink from 2120 until 2200 (Fig. 5). In contrast, the global mean tree cover continues to expand. From 2200 onwards, the global mean vegetation cover tends to stabilise. After the retreat of deserts in the Sahara, Arabia, and Australia until 2120, grass cover declines from 2120 until 2300 leading to an enlarged desert cover in these regions (Fig. 7). Tree cover further extends northward at the expense of the tundra. Tree cover increase is strongest in Alaska, where trees replace shrubs and grass. However, tree cover declines in eastern Europe and western Russia. In contrast, tree cover shrinks in the taiga region since precipitation declines. This northward shift of the boreal forest has also been found by Notaro et al. (2007) and O'ishi and Abe-Ouchi (2009).

The influence of vegetation dynamics on anthropogenic climate change

U. Port et al.

Title Page

Abstract

Introduction

Conclusions

References

Tables

Figures

⏪

⏩

◀

▶

Back

Close

Full Screen / Esc

Printer-friendly Version

Interactive Discussion



In response to intensified precipitation rates in southern South America even after 2120, tree cover proceeds to increase in this region. Thus, a bipolar pattern occurs in South America by 2300, with reduced tree cover in the north and extended tree cover in the south.

5 Compared to the period from 1850 until 2120, CO₂ fertilisation weakens after CO₂ emissions cease. Thus, climate change and weakening CO₂ fertilisation affect the terrestrial biosphere after the year 2120. Especially the vegetation in the desert regions responds to the weakening of the CO₂ fertilisation. In the Sahara, stronger water stress, initiated by decreased precipitation, adds to this effect (Fig. 9). The decline in precipita-
10 tion rate which is visible around 2100 continues leading to a 35 % smaller precipitation rate in 2300 in the DYN simulation than in the control run. Other than in the control simulation, grass and shrubs are unable to survive in the DYN simulation due to stronger water stress and weaker CO₂ fertilisation. Thus, the desert area extends from 77 % in 1850 to 82 % in 2300. In contrast, tree cover still persists indicating that trees are
15 less sensitive to CO₂ fertilisation than grass. Furthermore, trees can better survive the lower precipitation rates than shrubs.

3.3 Impact of dynamic vegetation on climate around 2300

The impact of vegetation dynamics on climate can be assessed by comparing the DYN and the STAT simulation. It can be seen that natural vegetation cover shifts leads to
20 a higher atmospheric CO₂ concentration by 37 ppm and a lower global mean temperature by 0.22 K averaged over the years from 2270 until 2299 (Fig. 2). On a regional scale, temperature in the DYN simulation is lower in South America, Alaska, northern Africa, and parts of Asia than in the STAT simulation. Differences in the annual mean precipitation on a regional and a global scale are negligibly small.

The influence of vegetation dynamics on anthropogenic climate change

U. Port et al.

Title Page

Abstract

Introduction

Conclusions

References

Tables

Figures



Back

Close

Full Screen / Esc

Printer-friendly Version

Interactive Discussion



3.3.1 Biogeophysical effect of vegetation dynamics on climate

In order to separate the biogeophysical effect from the net effect of biogeographical changes on climate, the differences between the DYN and the STAT_PS simulations are analysed in this subsection.

5 The biogeophysical effect of vegetation cover change has no significant effect on global annual mean temperature, but has an impact on regional climate change (Fig. 11). Compared to the STAT_PS simulation, annual mean temperature is higher in Eastern Europe, Siberia, around the Hudson Bay, and in the Amazon region and it is lower in southern South Africa in the DYN simulation.

10 Tree cover increases in the northern high latitudes until 2300. The biogeophysical effect of the expanding tree cover is a regional warming over land. Thereby, two components of the energy budget are affected. Compared to the STAT_PS simulation, evapotranspiration rates over land and thus latent heat flux are larger in the DYN simulation. The maximum evapotranspiration increase occurs in summer (Fig. 13) as trees carry a maximum amount of leaves in this time. The resultant impact on continental temperature is evident in the annual cycle of temperature differences between the DYN and the STAT_PS simulation, as the strongest cooling occurs in May and July.

15 Besides higher evapotranspiration, expanded boreal forests leads to a lower regional land surface albedo and thus higher net shortwave radiation in the DYN than in the STAT_PS simulation. The resulting regional warming over land depends strongly on the season (Fig. 13). From June until October, surface albedo differences between the DYN and the STAT_PS simulation caused by the darker colour of trees compared to grass and shrubs are small. However, in late winter and early spring, a strong albedo reduction occurs. The dominant effect causing this decline is the snow-masking effect of trees. Even for deciduous trees, dark trunks, branches, and twigs mask the snow and thus lead to a lower albedo (Bergengren et al., 2001; Bonan, 2008). The snow-masking effect is strong in spring, when snow still covers the ground and insolation increases.

20

25

The influence of vegetation dynamics on anthropogenic climate change

U. Port et al.

Title Page

Abstract

Introduction

Conclusions

References

Tables

Figures



Back

Close

Full Screen / Esc

Printer-friendly Version

Interactive Discussion



Thus, the snow-masking effect leads to the higher April temperatures over land in the DYN than in the STAT_PS simulation.

In the annual mean, the effect of reduced land surface albedo in spring outweighs the effect of increased latent heat flux in summer. Thus, the biogeophysical effect of extended tree growth in the northern high latitudes is a warming over land of 0.13 K (DYN – STAT_PS). These results agree with Levis et al. (1999) who find the same counteracting effects of higher evapotranspiration rates and lower surface albedo due tree cover expansion in the northern high latitudes.

The biogeophysical effect of vegetation cover shifts on climate in the Amazon region is a warming. Compared to the STAT_PS simulation, tree cover is smaller in the DYN simulation leading less evapotranspiration. Thus, sensible heat flux is increased and cloud cover is decreased. Higher sensible heat flux in the DYN simulation results in higher temperatures than in the STAT_PS simulation. The smaller cloud cover leads to a cooling since the loss of thermal radiation is larger and thus net long wave radiation is smaller. However, the cooling due to the smaller cloud cover is weaker than the warming due to the decrease in latent heat flux. In sum, the biogeophysical effect causes a warming in the Amazon region. This result differs from previous ones. While we find an impact of declined tree cover on temperature in the Amazon region, Cox et al. (2004) suggest that a forest dieback results in reduced precipitation rates and leaves temperature unaffected. The decline in tree cover suggested by Cox et al. (2004) is stronger than in our results. Therefore a weaker response in precipitation is plausible. Why the results differ for temperature changes remains unclear.

Changes in vegetation cover are small in the Sahara/Sahel compared to the Amazon region and the northern high latitudes (Fig. 9). Therefore, the biogeophysical effect on climate is weak in this region. Differences in precipitation and evapotranspiration occur, but fluctuate, and no significant effect of dynamic vegetation on precipitation can be identified.

The influence of vegetation dynamics on anthropogenic climate change

U. Port et al.

Title Page

Abstract

Introduction

Conclusions

References

Tables

Figures



Back

Close

Full Screen / Esc

Printer-friendly Version

Interactive Discussion



3.3.2 Biogeochemical effect of vegetation dynamics on climate

Comparing the carbon storage on the land, in the ocean, and in the atmosphere in the DYN and in the STAT simulation illustrates the impact of vegetation dynamics on the carbon cycle. Until the year 2120, the impact of vegetation cover shifts on the carbon cycle is weak (Fig. 15) since no differences in land, ocean, and atmosphere carbon storage between the DYN and the STAT simulation occur. However, vegetation dynamics clearly influence the global carbon budget after the emissions cease. After 2120, the land and the ocean take up carbon from the atmosphere in both simulation, DYN and STAT. Though, in the DYN simulation the land carbon uptake is higher. Land stores 39 % of the anthropogenic CO₂ emissions in the DYN simulation in 2300 (in STAT land stores 35 %) resulting in less carbon to be left in the atmosphere, and thus, a weaker radiative forcing than in the STAT simulation.

Changes in the geographical distribution of carbon storage due to vegetation dynamics are consistent with tree cover changes (Fig. 14). In agreement with Jones et al. (2010), a larger boreal forest extension in the DYN simulation than in the STAT simulation leads to an additional terrestrial carbon storage in the northern high latitudes. The carbon storage is increased in the south and decreased in the north of South America, as the tropical trees shift southward. In the continental interior arid regions, the carbon storage is equal in the DYN and in the STAT simulation. Since tree cover in the Sahel zone spreads in the DYN simulation, regional carbon storage is slightly larger than in the STAT simulation. In summary, the extended global mean global tree cover leads to an increase in total carbon storage on land by 11 %.

The additional land carbon uptake due to biogeographical shifts leads to a 37 ppm lower atmospheric CO₂ concentration in the DYN simulation compared to the STAT simulation (Fig. 2). This biogeochemical effect results in a cooler global climate. Assuming a linear relationship between atmospheric CO₂ concentration and global mean temperature, climate sensitivity can be estimated by calculating the ratio of the temperature change to the increase in atmospheric CO₂ concentration (Friedlingstein et al., 2006).

The influence of vegetation dynamics on anthropogenic climate change

U. Port et al.

Title Page

Abstract

Introduction

Conclusions

References

Tables

Figures



Back

Close

Full Screen / Esc

Printer-friendly Version

Interactive Discussion



**The influence of
vegetation dynamics
on anthropogenic
climate change**

U. Port et al.

Title Page

Abstract

Introduction

Conclusions

References

Tables

Figures

◀

▶

◀

▶

Back

Close

Full Screen / Esc

Printer-friendly Version

Interactive Discussion



For the STAT simulation, climate sensitivity equals $5.1 \text{ K}/707 \text{ ppm} = 0.0072 \text{ K ppm}^{-1}$. Thus, the lower atmospheric CO_2 concentration of 37 ppm due to the biogeochemical effect of dynamic vegetation is consistent with a cooling of approximately 0.27 K.

As presented earlier in this section, the biogeophysical effect of vegetation cover shifts has no significant effect on the global climate. However, the net effect of vegetation dynamics is a slight cooling by 0.22 K by 2300. Thus, the biogeochemical effect is the dominant effect on the time scale of centuries and attenuates anthropogenic climate change.

We would like emphasise upon the fact that natural vegetation cover changes are analysed in this study and changes in the vegetation cover due to land-use are neglected. For instance, considering regional transition from forest to crop land would likely lead to a different impact of vegetation cover changes on climate than estimated here.

4 Conclusions

Changes in the natural vegetation cover and their impact on climate have been assessed for a CO_2 emission scenario which combines RCP 8.5 scenario until the year 2120 and zero emissions from 2120 until 2300. The used Earth System Model, MPI ESM, includes an interactive carbon cycle and dynamic vegetation. Both, biogeophysical and biogeochemical effects of vegetation are taken into account and are analysed separately.

The terrestrial biosphere strongly responds to simulated climate changes and elevated atmospheric CO_2 . We find that, in agreement with previous studies (Notaro et al., 2007; O'ishi and Abe-Ouchi, 2009), global mean vegetation expands. On global average, tree and grass coverage increase until 2120, while shrub coverage and the area not covered by vegetation decline. After 2120, tree coverage continues increasing, shrub coverage persists to decrease, and grass coverage decreases. The area not covered by vegetation increases after 2120, when the emissions are set to zero.

At the end of the simulation, the area not covered by vegetation is smaller than in the pre-industrial state.

In the northern high latitudes, trees benefit from the prolonged growing season and extend northward into the tundra region. In contrast, at the southern border of the taiga region, warming and resultant increased water stress causes tree cover to decline by 2300. In the subtropical desert areas, vegetation cover increases due to CO₂ fertilisation and enhanced water-use efficiency until 2120. After the emissions cease and atmospheric CO₂ concentration declines, desert area extends again since CO₂ fertilisation weakens. In the Sahara, decreased precipitation suppresses greening even before 2120. Until the year 2090, precipitation increases in the Sahara region, but afterwards it declines. Resulting drying leads to an expansion of the desert area. In the Amazon region, a decline in tree cover is found, although not as strong as suggested by Betts et al. (2004). We find a decrease in tree cover by 13 % absolute coverage in this region.

Changes in vegetation cover influence the regional climate by affecting regional energy, heat, and moisture fluxes. In the northern high latitudes, increased tree cover leads to a lower surface albedo and higher evapotranspiration rates in the simulation with dynamic vegetation than in the simulation with the static vegetation cover. These two modifications have a counteracting effect on the regional temperature depending on the season. A reduced surface albedo leads to a warming, while increased evapotranspiration causes a cooling. In the annual mean, the warming due to the lower albedo overcompensates the cooling due to enhanced evapotranspiration. The biogeophysical effect of extended tree cover leads to a warming of 0.13 K in this region. In the Amazon region, the biogeophysical effect of reduced tree cover results in lower evapotranspiration rates and leads to a regional warming since the latent heat flux is reduced. On a global scale, no significant change in climate due to the biogeophysical effect of vegetation dynamics is found.

Extended global mean vegetation cover results in an increased land carbon storage by 11 % in the simulation with dynamic vegetation compared to the simulation with the

The influence of vegetation dynamics on anthropogenic climate change

U. Port et al.

Title Page

Abstract

Introduction

Conclusions

References

Tables

Figures



Back

Close

Full Screen / Esc

Printer-friendly Version

Interactive Discussion



static pre-industrial vegetation cover. Thus, by 2300, atmospheric CO₂ concentration is reduced by 37 ppm due to vegetation dynamics. Hence, the biogeochemical effect of vegetation leads to a global cooling. The net effect of vegetation cover changes (biogeophysical plus biogeochemical) on the global climate is a cooling by 0.22 K by 2300. Since the impact of the biogeophysical effect on the global climate is marginal, the biogeochemical effect is the dominant effect on the time scale of centuries. The increased land carbon uptake due to vegetation dynamics leads to a cooler climate and attenuates anthropogenic climate change.

Acknowledgements. We would like to thank Veronika Gayler for the technical support, Thomas Raddatz for comments on the manuscript as well as our anonymous reviewers.

References

- Bala, G., Caldeira, K., Mirin, A., Wickett, M., Delire, C., and Phillips, T. J.: Biogeophysical effects of CO₂ fertilization on global climate, *Tellus B*, 58, 620–627, 2006. 494
- Bala, G., Caldeira, K., Wickett, M., Phillips, T. J., and Lobell, D. B.: Combined climate and carbon-cycle effects of large-scale deforestation, *P. Natl. Acad. Sci. USA*, 104, 6550–6555, 2007. 488
- Bathiany, S., Claussen, M., Brovkin, V., Raddatz, T., and Gayler, V.: Combined biogeophysical and biogeochemical effects of large-scale forest cover changes in the MPI earth system model, *Biogeosciences*, 7, 1383–1399, doi:10.5194/bg-7-1383-2010, 2010. 488
- Beck, P. S. A. and Goetz, S.: Satellite observations of high northern latitude vegetation productivity changes between 1982 and 2008: ecological variability and regional differences, *Environ. Res. Lett.*, 6, 045501, doi:10.1088/1748-9326/6/4/045501, 2011. 487
- Bergengren, J. C., Thompson, S. L., Pollard, D., and DeConto, R. M.: Modeling global climate-vegetation interactions in a doubled CO₂ world, *Climatic Change*, 50, 31–75, 2001. 497
- Betts, R. A., Cox, P. M., Collins, M., Harris, P. P., Huntingford, C., and Jones, C. D.: The role of ecosystem-atmosphere interactions in simulated Amazonian precipitation decrease and forest dieback under global climate warming, *Theor. Appl. Climatol.*, 78, 157–175, 2004. 489, 493, 501

The influence of vegetation dynamics on anthropogenic climate change

U. Port et al.

Title Page

Abstract

Introduction

Conclusions

References

Tables

Figures



Back

Close

Full Screen / Esc

Printer-friendly Version

Interactive Discussion



**The influence of
vegetation dynamics
on anthropogenic
climate change**

U. Port et al.

[Title Page](#)[Abstract](#)[Introduction](#)[Conclusions](#)[References](#)[Tables](#)[Figures](#)[⏪](#)[⏩](#)[◀](#)[▶](#)[Back](#)[Close](#)[Full Screen / Esc](#)[Printer-friendly Version](#)[Interactive Discussion](#)

- Bonan, G. B.: Forests and climate change: Forcings, feedbacks, and the climate benefits of forests, *Science*, 320, 1444–1449, 2008. 497
- Brovkin, V.: Climate-vegetation interaction, *Journal de Physique IV*, 12, 57–72, 2002. 488
- Brovkin, V., Raddatz, T., and Reick, C. H.: Global biogeophysical interactions between forest and climate, *Geophys. Res. Lett.*, 36, L07405, doi:10.1029/2009GL037543, 2009. 488, 490
- 5 Claussen, M., Brovkin, V., and Ganopolski, A.: Biogeophysical versus biogeochemical feedbacks of large-scale land cover change, *Geophys. Res. Lett.*, 28, 1011–1014, 2001. 487, 488
- Cox, P. M., Betts, R. A., Collins, M., Harris, P. P., Huntingford, C., and Jones, C. D.: Amazonian forest dieback under climate-carbon cycle projections for the 21st century, *Theor. Appl. Climatol.*, 78, 137–156, 2004. 489, 498
- 10 de Boera, H. J., Lammertsma, E. I., Wagner-Cremer, F., Dilcher, D. L., Wassena, M. J., and Dekker, S. C.: Climate forcing due to optimization of maximal leaf conductance in subtropical vegetation under rising CO₂, *P. Natl. Acad. Sci.*, 108, 4041–4046, 2011. 487
- 15 Essery, R., Rutter, N., Pomeroy, J., Baxter, R., and Stahli, M.: An evaluation of forest snow process simulations, *B. Am. Meteorol. Soc.*, 90, 1120, doi:10.1175/2009BAMS2629.1, 2009. 488
- Friedlingstein, P., Cox, P., Betts, R., Bopp, L., von Bloh, W., Brovkin, V., Cadule, P., Doney, S., Eby, M., Fung, I., Bala, G., John, J., Jones, C., Joos, F., Kato, T., Kawamiya, M., Knorr, W., Lindsay, K., Matthews, H. D., Raddatz, T., Rayner, P., Reick, C., Roeckner, E., Schnitzler, K.-G., Schnur, R., Strassmann, K., Weaver, A. J., Yoshikawa, C., and Zeng, N.: Climate-carbon cycle feedback analysis, results from the C⁴MIP model intercomparison, *J. Climate*, 19, 3337–3353, 2006. 499
- 20 Jones, C., Liddicoat, S., and Lowe, J.: Role of terrestrial ecosystems in determining CO₂ stabilization and recovery behaviour, *Tellus B*, 62, 682–699, 2010. 488, 499
- Jungclaus, J. H., Keenlyside, N., Botzet, M., Haak, H., Luo, J. J., Latif, M., Marotzke, J., Mikolajewicz, U., and Roeckner, E.: Ocean circulation and tropical variability in the coupled model ECHAM5/MPI-OM, *J. Climate*, 19, 3952–3972, 2006. 490
- Levis, S., Foley, J. A., and Pollard, D.: CO₂, climate, and vegetation feedbacks at the last glacial maximum, *J. Geophys. Res.-Atmos.*, 104, 31191–31198, 1999. 498
- 30 McBean, G., Alekseev, G., Chen, D., Forland, E., Fyfe, J., Groisman, P. Y., King, R., Melling, H., Vose, R., and Whitfield, P. H.: Arctic climate impact assessment, chapter 2, Cambridge University Press, 21–60, 2005. 492

The influence of vegetation dynamics on anthropogenic climate change

U. Port et al.

Title Page

Abstract

Introduction

Conclusions

References

Tables

Figures

⏪

⏩

◀

▶

Back

Close

Full Screen / Esc

Printer-friendly Version

Interactive Discussion



- Meehl, G. A., Stocker, T. F., Collins, W. D., Friedlingstein, P., Gaye, A. T., Gregory, J. M., Kitoh, A., Knutti, R., Murphy, J. M., Noad, A., Raper, S. C. B., Watterson, I. G., Weaver, A. J., and Zhao, Z.-C.: Global Climate Projections. in: *Climate Change 2007: The physical science basis, Contribution of Working Group I to the Fourth Assessment Report of the Intergovernmental Panel on Climate Change*, Cambridge University Press, 747–845, 2007. 486, 492
- 5 Menzel, A. and Fabian, P.: Growing season extended in Europe, *Nature*, 397, 659–659, 1999. 487
- Myneni, R. B., Keeling, C. D., Tucker, C. J., Asrar, G., and Nemani, R. R.: Increased plant growth in the northern high latitudes from 1981 to 1991, *Nature*, 386, 698–702, 1997. 487
- 10 Notaro, M., Vavrus, S., and Liu, Z.: Global vegetation and climate change due to future increases in CO₂ as projected by a fully coupled model with dynamic vegetation, *J. Climate*, 20, 70–90, 2007. 488, 489, 494, 495, 500
- O’ishi, R. and Abe-Ouchi, A.: Influence of dynamic vegetation on climate change arising from increasing CO₂, *Clim. Dynam.*, 33, 645–663, 2009. 488, 494, 495, 500
- 15 Piao, S., Wang, X., Ciais, P., Zhu, B., and Wang, T.: Changes in satellite-derived vegetation growth trend in temperate and boreal Eurasia from 1982 to 2006, *Global Change Biol.*, 17, 3228–3239, 2011. 487
- Raddatz, T. J., Reick, C. H., Knorr, W., Kattge, J., Roeckner, E., Schnur, R., Schnitzler, K.-G., Wetzels, P., and Jungclaus, J.: Will the tropical land biosphere dominate the climate-carbon cycle feedback during the twenty-first century?, *Clim. Dynam.*, 29, 565–574, 2007. 489
- 20 Roeckner, E., Brokopf, R., Esch, M., Giorgette, M., Hagemann, S., Kornblueh, L., Manzini, E., Schlese, U., and Schulzweida, U.: The general circulation model ECHAM5, Part I: Model description, Report 349, Max-Planck-Institut for Meteorology, Hamburg, 2003. 489
- Snyder, P. K., Delire, C., and Foley, J. A.: Evaluating the influence of different vegetation biomes on the global climate, *Clim. Dynam.*, 23, 279–302, 2004. 487
- 25 Wetzels, P., Winguth, A., and Maier-Reimer, E.: Sea-to-air CO₂ flux from 1948 to 2003: A model study, *Global Biogeochem. Cy.*, 19, GB2005, doi:10.1029/2004GB002339, 2005. 490
- Woodward, F. I. and Beerling, D. J.: The dynamics of vegetation change: health warnings for equilibrium ‘dodo’ models, *Global Ecol. Biogeogr. Lett.*, 6, 413–418, 1997. 486
- 30 Yurova, A. Y. and Volodin, E. M.: Coupled simulation of climate and vegetation dynamics, *Izvestiya, Atmos. Ocean. Phys.*, 47, 531–539, 2011. 488, 489

Zhou, L. M., Tucker, C. J., Kaufmann, R. K., Slaybackd, D., and Shabanov, N. V.: Variations in northern vegetation activity inferred from satellite data of vegetation index during 1981 to 1999, *J. Geophys. Res.*, 106, 20069–20083, 2001. 487

ESDD

3, 485–522, 2012

The influence of vegetation dynamics on anthropogenic climate change

U. Port et al.

Title Page

Abstract

Introduction

Conclusions

References

Tables

Figures



Back

Close

Full Screen / Esc

Printer-friendly Version

Interactive Discussion



The influence of vegetation dynamics on anthropogenic climate change

U. Port et al.

Title Page

Abstract

Introduction

Conclusions

References

Tables

Figures

◀

▶

◀

▶

Back

Close

Full Screen / Esc

Printer-friendly Version

Interactive Discussion

Table 1. Plant functional types defined in JSBACH.

Vegetation cover type	Plant functional type
trees	tropical evergreen forest tropical deciduous forest extra-tropical evergreen forest extra-tropical deciduous forest
shrubs	raingreen shrubs cold shrubs
grass	C ₃ grass C ₄ grass

The influence of vegetation dynamics on anthropogenic climate change

U. Port et al.

Table 2. Experimental setup. The used CO₂ emission scenario is based on the RCP 8.5.

Simulation	Period	Vegetation cover	CO ₂ forcing
CTL	1700–2300	dynamic	no anthropogenic CO ₂ emissions
STAT	1850–2300	static	CO ₂ emissions according to RCP 8.5
DYN	1850–2300	dynamic	CO ₂ emissions according to RCP 8.5
STAT_PS	1850–2300	static	atm. CO ₂ content set to the values simulated in DYN

Title Page

Abstract

Introduction

Conclusions

References

Tables

Figures

⏪

⏩

◀

▶

Back

Close

Full Screen / Esc

Printer-friendly Version

Interactive Discussion



The influence of vegetation dynamics on anthropogenic climate change

U. Port et al.

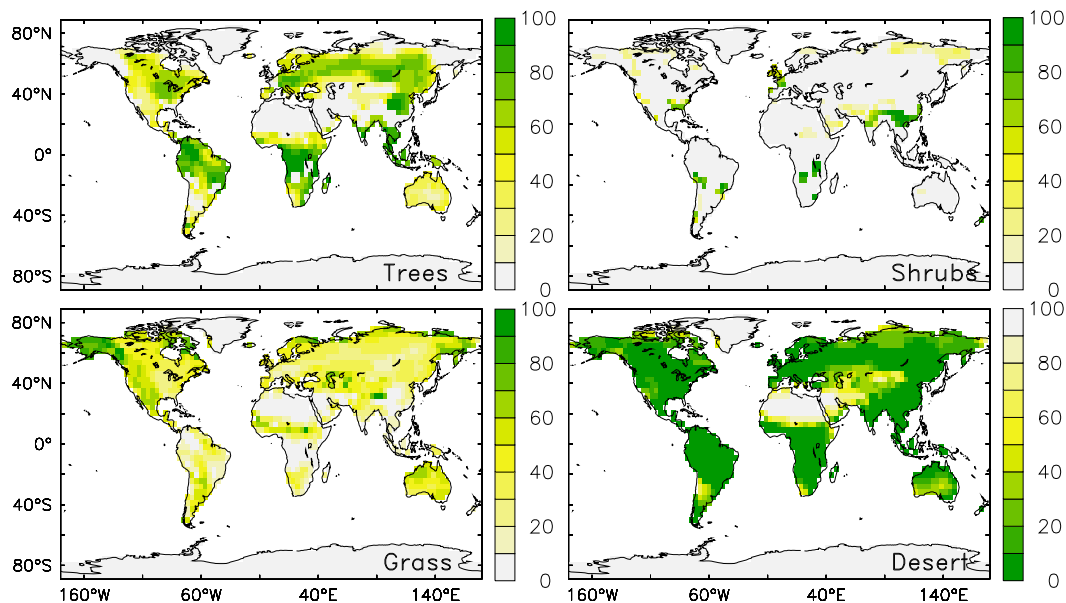


Fig. 1. Equilibrium vegetation distribution of the CTL simulation in [%], averaged over 50 yr. Trees include tropical evergreen and deciduous forest as well as extra-tropical evergreen and deciduous forest. Grass comprises C_3 grass and C_4 grass, while shrubs include raingreen and cold shrubs. Bare areas are interpreted as desert.

Title Page

Abstract

Introduction

Conclusions

References

Tables

Figures

◀

▶

◀

▶

Back

Close

Full Screen / Esc

Printer-friendly Version

Interactive Discussion

**The influence of
vegetation dynamics
on anthropogenic
climate change**

U. Port et al.

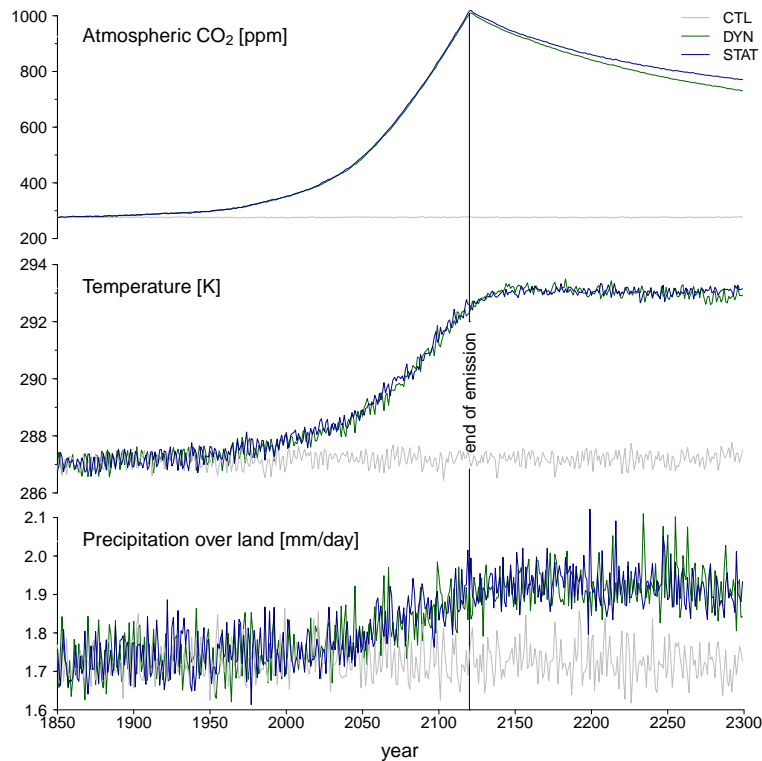


Fig. 2. Time series of annual mean atmospheric CO₂ concentration, global annual mean temperature, and annual mean precipitation averaged over total land area for the CTL (grey line), DYN (green line), and STAT (blue line) simulation.

[Title Page](#)[Abstract](#)[Introduction](#)[Conclusions](#)[References](#)[Tables](#)[Figures](#)[◀](#)[▶](#)[◀](#)[▶](#)[Back](#)[Close](#)[Full Screen / Esc](#)[Printer-friendly Version](#)[Interactive Discussion](#)

The influence of vegetation dynamics on anthropogenic climate change

U. Port et al.

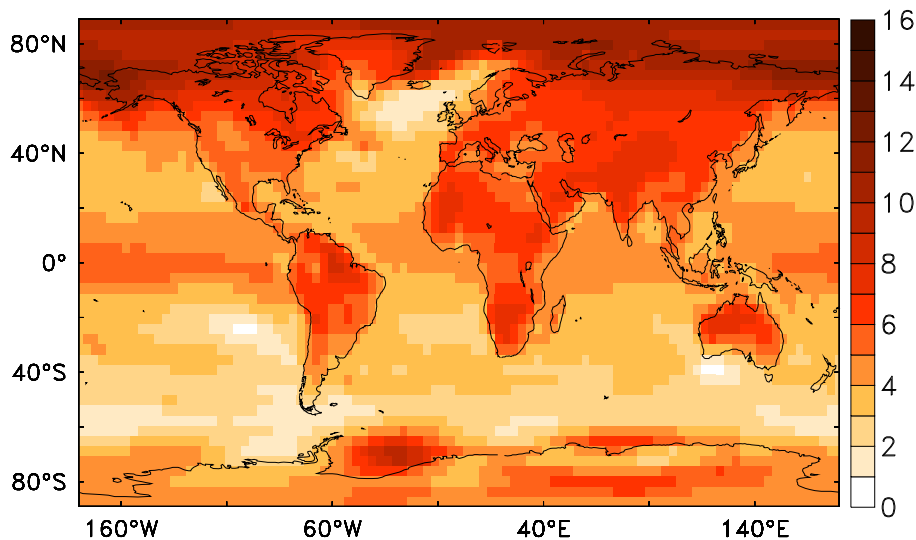


Fig. 3. Differences in annual mean temperature caused by anthropogenic CO₂ emissions and vegetation dynamics in [K] (DYN – CTL) averaged between the years 2090 and 2119. Shown differences are significant on a 95 % level of significance.

Title Page

Abstract

Introduction

Conclusions

References

Tables

Figures

⏪

⏩

◀

▶

Back

Close

Full Screen / Esc

Printer-friendly Version

Interactive Discussion

**The influence of
vegetation dynamics
on anthropogenic
climate change**

U. Port et al.

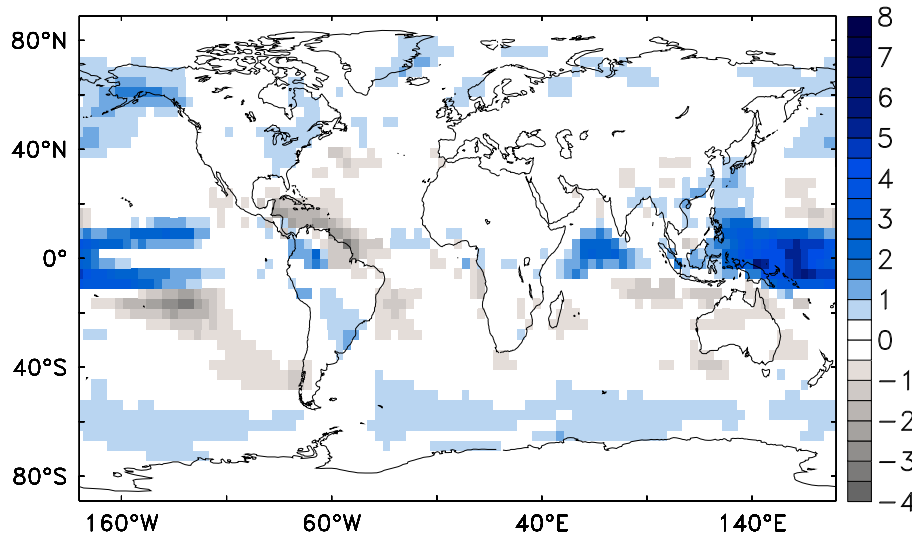


Fig. 4. Differences in annual mean precipitation caused by anthropogenic CO₂ emissions and vegetation dynamics in [mm day⁻¹] (DYN – CTL) averaged between the years 2090 and 2119. Shown differences are significant on a 95 % level of significance.

[Title Page](#)[Abstract](#)[Introduction](#)[Conclusions](#)[References](#)[Tables](#)[Figures](#)[⏪](#)[⏩](#)[◀](#)[▶](#)[Back](#)[Close](#)[Full Screen / Esc](#)[Printer-friendly Version](#)[Interactive Discussion](#)

The influence of vegetation dynamics on anthropogenic climate change

U. Port et al.

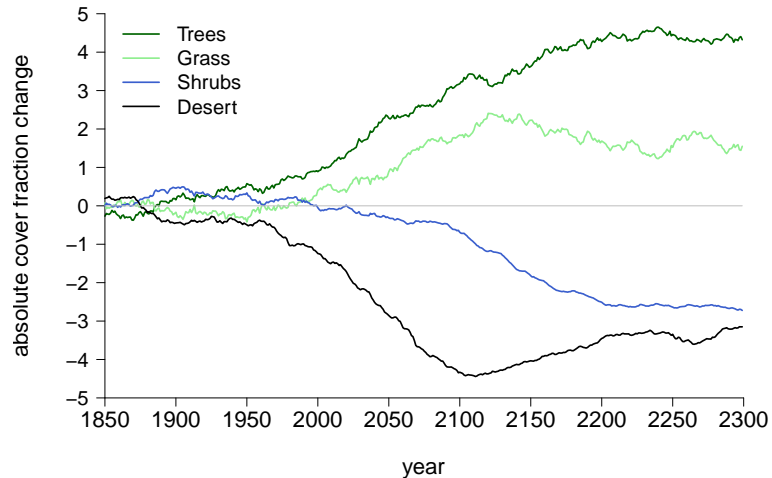


Fig. 5. Time series of changes in absolute global mean vegetation cover (DYN – CTL) in [%]. Forest includes tropical evergreen and deciduous trees as well and extra-tropical evergreen and deciduous trees, while shrubs contain cold and raingreen shrubs and grass includes C₃ and C₄ grass.

[Title Page](#)
[Abstract](#)
[Introduction](#)
[Conclusions](#)
[References](#)
[Tables](#)
[Figures](#)
[⏪](#)
[⏩](#)
[◀](#)
[▶](#)
[Back](#)
[Close](#)
[Full Screen / Esc](#)
[Printer-friendly Version](#)
[Interactive Discussion](#)

The influence of vegetation dynamics on anthropogenic climate change

U. Port et al.

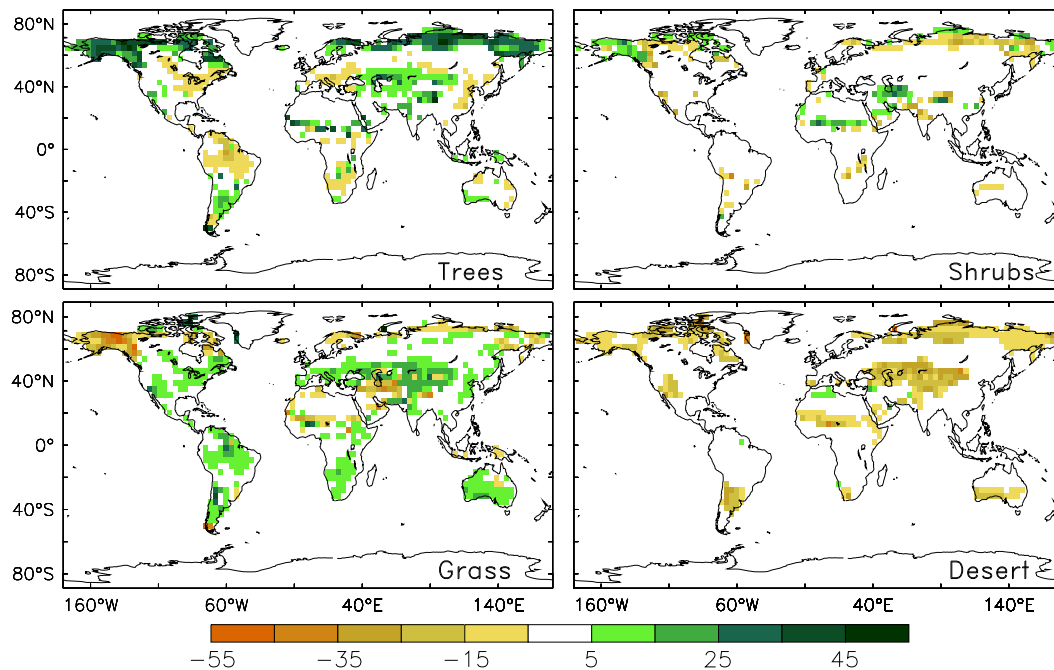


Fig. 6. Differences in absolute vegetation cover between the DYN and the CTL simulation averaged between the years 2090 until 2119 given in [%].

Title Page

Abstract

Introduction

Conclusions

References

Tables

Figures

◀

▶

◀

▶

Back

Close

Full Screen / Esc

Printer-friendly Version

Interactive Discussion

The influence of vegetation dynamics on anthropogenic climate change

U. Port et al.

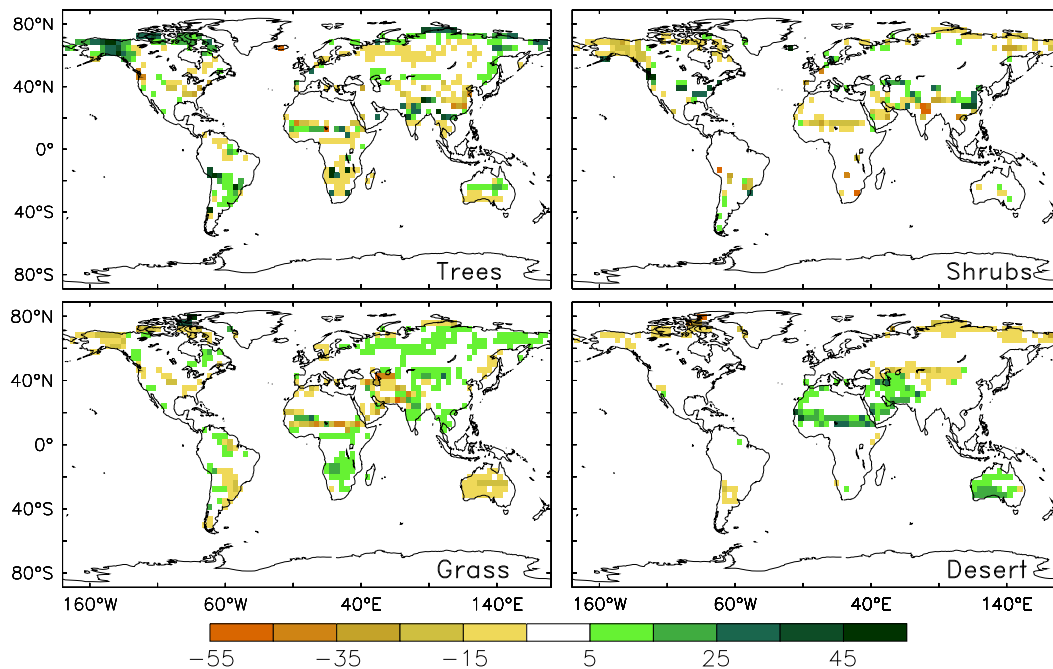


Fig. 7. Changes in absolute vegetation cover in [%] from 2120 (averaged between 2090 and 2119) until 2300 (averaged between 2270 and 2299).

[Title Page](#)[Abstract](#)[Introduction](#)[Conclusions](#)[References](#)[Tables](#)[Figures](#)[◀](#)[▶](#)[◀](#)[▶](#)[Back](#)[Close](#)[Full Screen / Esc](#)[Printer-friendly Version](#)[Interactive Discussion](#)

**The influence of
vegetation dynamics
on anthropogenic
climate change**

U. Port et al.

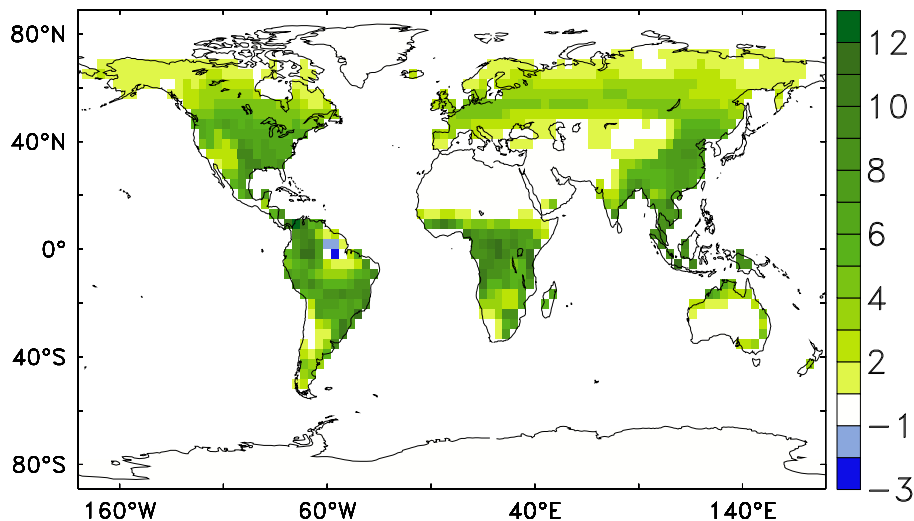


Fig. 8. Differences in Net Primary Productivity (NPP) caused by anthropogenic CO₂ emissions in [mol(C) m⁻² yr⁻¹] (STAT – CTL) averaged between the years 2090 and 2119.

[Title Page](#)[Abstract](#)[Introduction](#)[Conclusions](#)[References](#)[Tables](#)[Figures](#)[⏪](#)[⏩](#)[◀](#)[▶](#)[Back](#)[Close](#)[Full Screen / Esc](#)[Printer-friendly Version](#)[Interactive Discussion](#)

**The influence of
vegetation dynamics
on anthropogenic
climate change**

U. Port et al.

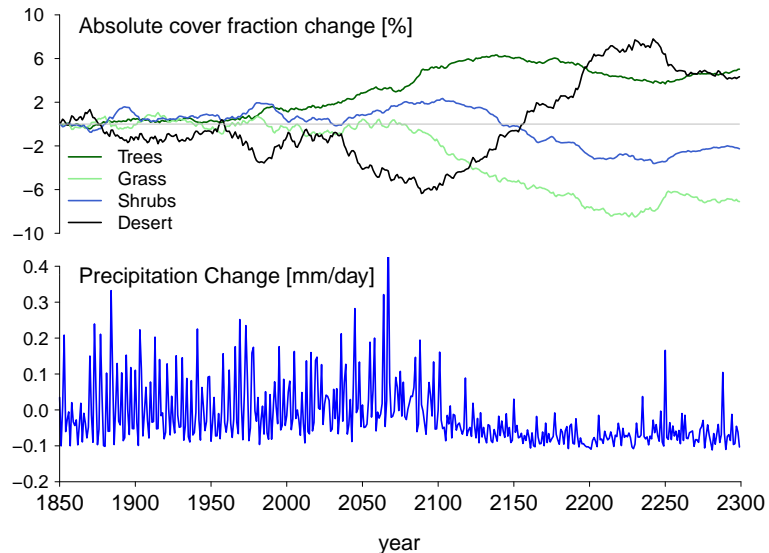


Fig. 9. Time series of differences in vegetation cover (top panel) and differences in annual mean precipitation due to anthropogenic climate change and vegetation cover change (DYN – CTL) (bottom panel) for the Sahara/Sahel region (20° W– 45° E and 10° N– 35° N).

The influence of vegetation dynamics on anthropogenic climate change

U. Port et al.

Title Page

Abstract

Introduction

Conclusions

References

Tables

Figures

⏪

⏩

◀

▶

Back

Close

Full Screen / Esc

Printer-friendly Version

Interactive Discussion

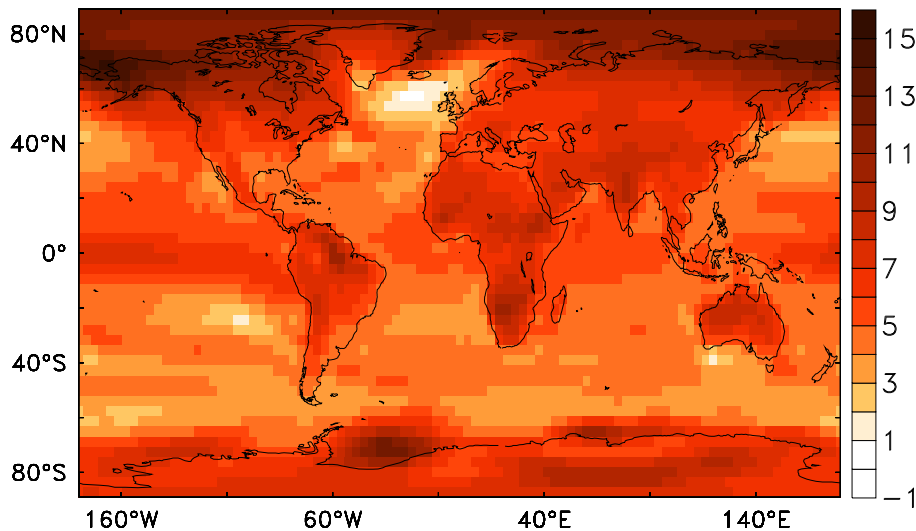


Fig. 10. Differences in annual mean temperature caused by anthropogenic CO₂ emissions and vegetation dynamics in [K] (DYN – CTL) averaged between the years 2070 and 2299. Shown differences are significant on a 95 % level of significance.

The influence of vegetation dynamics on anthropogenic climate change

U. Port et al.

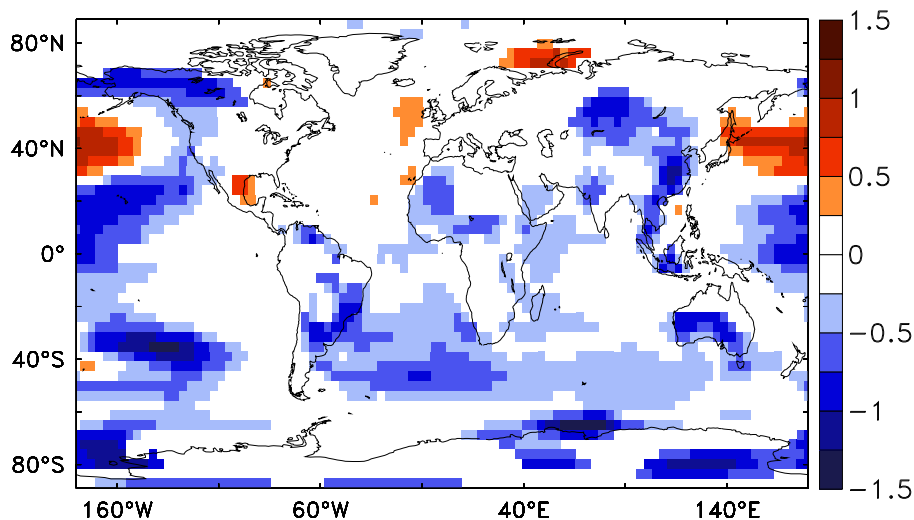


Fig. 11. Differences in annual mean temperature caused by the net effect of changes in vegetation cover in [K] (DYN – STAT) averaged between the years 2270 and 2299. Shown differences are significant on a 95 % level of significance.

[Title Page](#)[Abstract](#)[Introduction](#)[Conclusions](#)[References](#)[Tables](#)[Figures](#)[⏪](#)[⏩](#)[◀](#)[▶](#)[Back](#)[Close](#)[Full Screen / Esc](#)[Printer-friendly Version](#)[Interactive Discussion](#)

The influence of vegetation dynamics on anthropogenic climate change

U. Port et al.

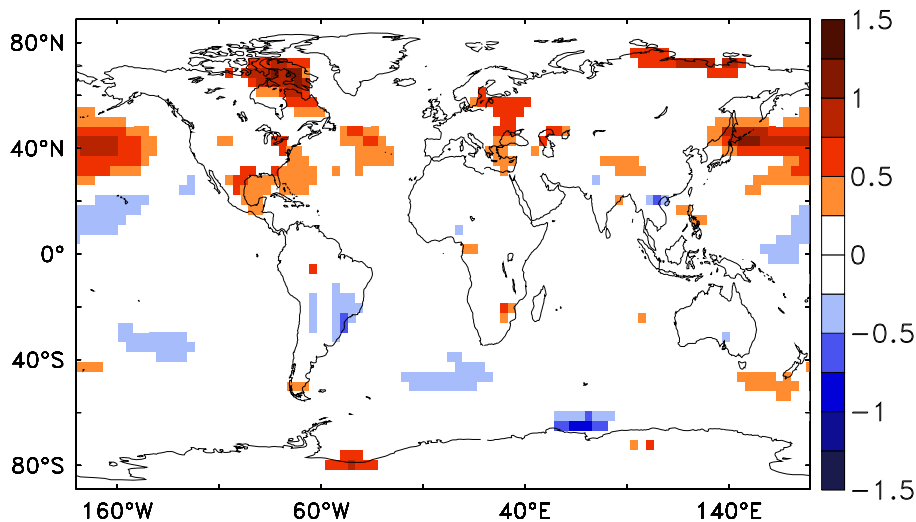


Fig. 12. Differences in annual mean temperature caused by biogeophysical effects of changes in vegetation cover in [K] (DYN – STAT_PS) averaged between the years 2270 and 2299. Shown differences are significant on a 95% level of significance.

[Title Page](#)[Abstract](#)[Introduction](#)[Conclusions](#)[References](#)[Tables](#)[Figures](#)[⏪](#)[⏩](#)[◀](#)[▶](#)[Back](#)[Close](#)[Full Screen / Esc](#)[Printer-friendly Version](#)[Interactive Discussion](#)

The influence of vegetation dynamics on anthropogenic climate change

U. Port et al.

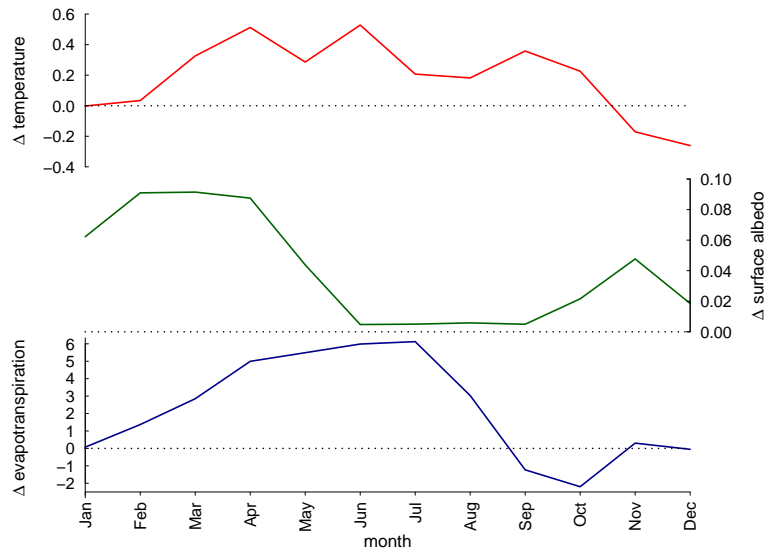


Fig. 13. Differences in the annual cycle of monthly mean surface albedo (green line), temperature in [K] (red line), and evapotranspiration in [10^7 mm day^{-1}] (blue line) in the northern high latitudes (60° N to 80° N , only land) caused by the biogeophysical effect of vegetation dynamics (DYN – STAT_PS) averaged between 2070 and 2299.

[Title Page](#)
[Abstract](#)
[Introduction](#)
[Conclusions](#)
[References](#)
[Tables](#)
[Figures](#)
[◀](#)
[▶](#)
[◀](#)
[▶](#)
[Back](#)
[Close](#)
[Full Screen / Esc](#)
[Printer-friendly Version](#)
[Interactive Discussion](#)

**The influence of
vegetation dynamics
on anthropogenic
climate change**

U. Port et al.

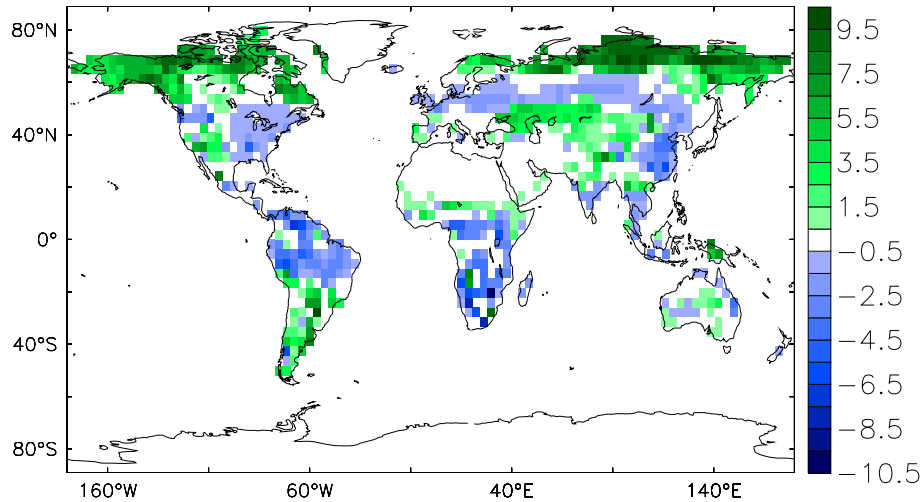


Fig. 14. Differences in total land carbon storage (sum of the biomass, soil, and litter pool) due to changes in vegetation cover in [kgC m^{-2}] (DYN – STAT) averaged between the years 2270 and 2300.

[Title Page](#)[Abstract](#)[Introduction](#)[Conclusions](#)[References](#)[Tables](#)[Figures](#)[⏪](#)[⏩](#)[◀](#)[▶](#)[Back](#)[Close](#)[Full Screen / Esc](#)[Printer-friendly Version](#)[Interactive Discussion](#)

The influence of vegetation dynamics on anthropogenic climate change

U. Port et al.

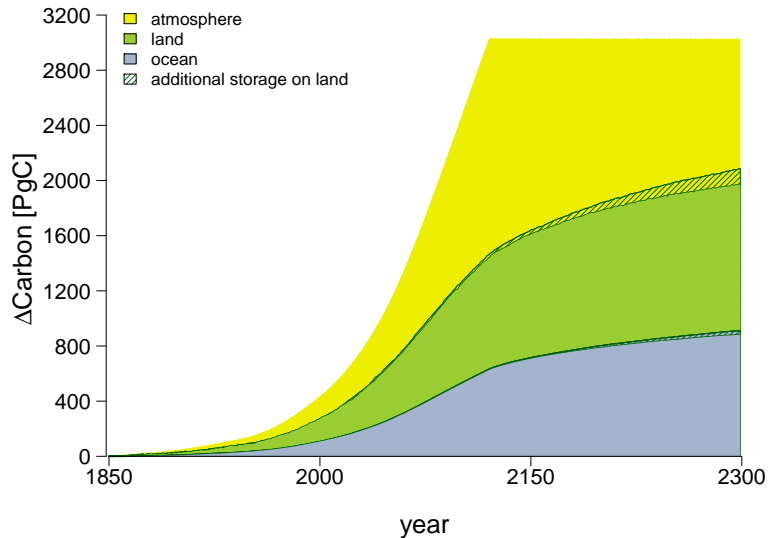


Fig. 15. Cumulated carbon budget simulated with the static pre-industrial vegetation cover. The shaded areas reflect the additional carbon storage on land due to vegetation cover changes. This additional land carbon storage leads to reduced carbon in the ocean (dark green shade over grey area) and in the atmosphere (dark green shade over yellow area).

Title Page

Abstract

Introduction

Conclusions

References

Tables

Figures

⏪

⏩

◀

▶

Back

Close

Full Screen / Esc

Printer-friendly Version

Interactive Discussion

